Application of FTIR spectroscopy to the characterization of archeological wood

Mohamed Traoré [a,*], Joeri Kaal [b], Antonio Martínez Cortizas [a]

[a] Departamento de Edafología y Química Agrícola, Facultad de Biología, Universidade de Santiago de Compostela, Campus Sur s/n, Santiago de Compostela 15782, Spain
[b] Instituto de Ciencias del Patrimonio (Incipit), Consejo Superior de Investigaciones Científicas (CSIC), San Roque 2, Santiago de Compostela 15704, Spain

ARTICLE INFO

ABSTRACT

Two archeological wood samples were studied by attenuated total reflectance Fourier transform infrared (FTIR–ATR) spectroscopy. They originate from a shipwreck in Ribadeo Bay in the northwest of Spain and from a beam wood of an old nave of the Cathedral of Segovia in the central Spain. Principal component analysis was applied to the transposed data matrix (samples as columns and spectral bands as rows) of 43 recorded spectra (18 in the shipwreck and 25 in the beam wood). The results showed differences between the two samples, with a larger proportion of carbohydrates and smaller proportion of lignin in the beam than in the shipwreck wood. Within the beam wood, lignin content was significantly lower in the recent than the old tree rings (P = 0.005). These variations can be attributed to species differences between the two woods (oak and pine respectively), with a mixture of guaiacyl and syringyl in hardwood lignin, whereas softwood lignin consists almost exclusively of guaiacyl moieties. The influence of environmental conditions on the FTIR fingerprint was probably reflected by enhanced oxidation of lignin in aerated conditions (beam wood) and hydrolysis of carbohydrates in submerged-anoxic conditions (shipwreck wood). Molecular characterization by analytical pyrolysis of selected samples from each wood type confirmed the interpretation of the mechanisms behind the variability in wood composition obtained by the FTIR–ATR.

© 2015 Elsevier B.V. All rights reserved.

1. Introduction

Fourier transform infrared (FTIR) spectroscopy is a useful analytical method for characterizing wood structural chemistry with minimal sample treatment [14,31]. This technique is based on molecular bond vibrations induced by infrared radiation. It is time-efficient and requires only small quantities of sample material [2,25]. FTIR spectroscopy is widely used in qualitative and also quantitative analysis of wood because of its ability to provide information about functional groups abundance and other specific structural features [1,4,6,11,32]. Popescu et al. [31] applied FTIR to assess variations in the relative proportions of carbohydrates and lignin in eucalyptus wood. Differences between trees from different species can often also be identified, such as hard- and softwood that can be distinguished from the relative proportions of polysaccharides and lignin [8,12,26,27], and from the larger abundance of methoxyl groups in hardwood than softwood lignin [7,42]; a mixture of guaiacyl (1-methoxy-2-hydroxyphenyl) and syringyl (1,3-dimethoxy-2-hydroxyphenyl) moieties is found in hardwood lignins whereas softwood lignin consist of virtually only of guaiacyl moieties [7,27].

Furthermore, FTIR spectroscopy has been used to characterize the chemical changes in wood that occur during weathering, chemical treatment and biodegradation processes [25,29]. Therefore, it can be applied to archeological wood samples to evaluate appropriate conservation methods. In addition, several studies have focused on the use of FTIR methodologies for studying wooden artifacts [29]. Popescu et al. [32] studied wood affected by fungi and found higher absorbance intensity of C–O bond vibration of oxidized lignin in decayed wood. However, as many absorbance bands can originate from more than one type of functional group, such as the presence of various vibration modes in carbohydrates and lignin at bands below 1460 cm^{-1} [27], the relation between FTIR spectral fingerprints and molecular structures present in the samples is not straightforward and requires isolating different signals from overlapping bands. This can be achieved by multivariate statistics.

Few studies have used multivariate statistics to unravel FTIR fingerprints, despite the potential of such an approach [6,18]. Principal component analysis (PCA) is among the more common multivariate methods applied to discriminate different bands related to molecular bond vibrations. PCA extracts the relevant absorbance regions, as shown by Xu et al. [40] with infrared data from wood. PCA on FTIR spectra was also of help to determine the larger proportion of cellulose in earlywood than in latewood [17], and to discriminate between softwood and hardwood based on their lignin composition [6]. In addition, trees from different environments could be distinguished using a combination of FTIR and PCA, identifying the influence of climatic factors and soil properties on wood chemistry [33,36]. This makes FTIR in

* Corresponding author.
E-mail addresses: traore.mohamed19@gmail.com (M. Traoré), joeri@samage.net (J. Kaal), antonio.martinez.cortizas@usc.es (A. Martínez Cortizas).

Fig. 1. Map showing the location of Segovia Cathedral and Ribadeo Bay.

combination with multivariate statistics a promising method for studying the provenance of archeological wood.

Pyrolysis–gas chromatography–mass spectrometry (PY–GC–MS) is based on thermal breakdown of relatively labile bonds under inert atmosphere (pyrolysis) followed by separation and identification of pyrolysis products by GC–MS. This technique allows distinguishing between guaiacyl and syringyl lignin moieties [34,38], and can also provide information on carbohydrate composition and the presence of other components such as extractives (tannins, resins, etc.). As such, PY–GC–MS provides complementary information on wood chemistry, which can lead to a better understanding of FTIR signatures.

The aim of this study was to characterize two different archeological woods using multivariate statistics on FTIR spectroscopy data. Pyrolysis–gas chromatography–mass spectrometry (PY–GC–MS) was applied to selected samples in order to obtain more detailed information on wood chemistry and aid in the identification of the main absorbance bands from the FTIR spectra.

2. Material and methods

2.1. Description of samples

Two archeological timbers of the 16th century were collected from Spain (Fig. 1). One of the woods corresponds to pine (*Pinus* cf. *sylvestris*) derived beam recovered from the roof of the nave of the Segovia Cathedral; after sawing, it was stored under dry conditions and ambient temperature in the laboratory. The other wood was taken from a shipwreck in Ribadeo Bay, taken during underwater archeological prospections in 2012. The shipwreck timber was made of oak (*Quercus* cf. *robur*) and was stored underwater in ambient temperature in the laboratory.

Before carrying out the analytical methods, the samples were oven dried at 30 °C for two weeks; afterwards their surfaces were cleaned in order to distinguish tree rings.

2.2. ATR–FTIR measurement

The infrared analytical technique was developed using a Varian 670-IR spectrometer (Varian Inc., Santa Clara, CA) equipped with an ATR device with a single-reflection diamond crystal (Pike GladiATR, Madison, WI). The spectra were collected in the absorbance range from 4000 to 400 cm^{-1} over 64 scans at a resolution of 4 cm^{-1}. The angle of incidence for the infrared beam through the diamond crystal was 45°.

FTIR–ATR analyses were done directly on the surface of the wood fragments, in consecutive positions from the outer (recent tree rings) to the inner part (old tree rings) of the wood fragments. Spectra were recorded in 25 positions in the beam wood, and in 18 in the shipwreck wood (Fig. 2). Although the infrared scanning was done in the region
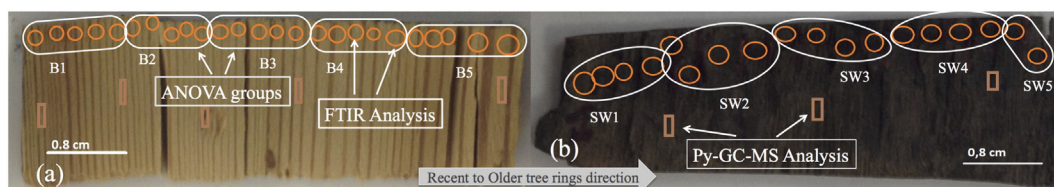

Fig. 2. Images of the two wood samples with the positions that were analyzed: the beam fragment (a) and the shipwreck fragment (b).
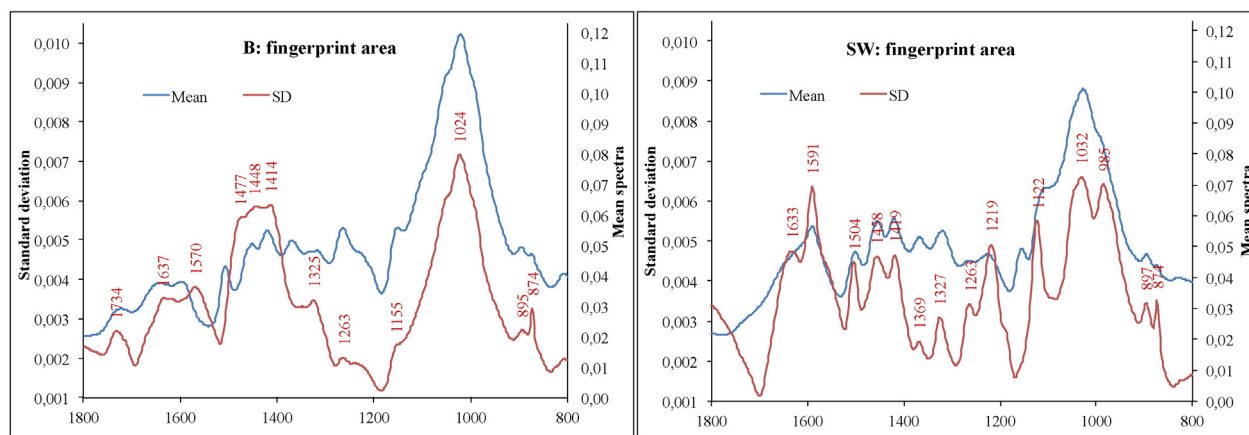
Fig. 3. Average and standard deviation of the FTIR spectra obtained in the archeological shipwreck (SW, $n = 18$) and beam (B, $n = 25$) wood, for the region between 1800 and 800 cm^{-1}.

between 4000 and 400 cm^{-1}, data evaluation was limited to the fingerprint region (1800–800 cm^{-1}), in which most of the variations of infrared absorption occur [4,26,28].

2.3. Data analysis

For a general description of the results average and standard deviation spectra were calculated for the two wood cores, whereas the detailed characterization of the spectral composition was done by applying principal component analysis (PCA). Besides the traditional PCA based on direct data matrices (samples as rows and spectral bands as columns), PCA on the transposed data matrix (samples as columns and spectral bands as rows) was performed to determine its ability to disentangle infrared spectra of wood. The transposed matrix focuses on the variation of the spectroscopic signal within the samples, providing an estimation of the statistical weight (i.e., loadings) of the main constituents of the samples. Using the direct data matrix, the

components are computed according to the variation of the absorbance frequency relative of each band in the samples, while in the transposed matrix the factors are computed according to the intensity of the absorbance relative to the whole spectrum. This approach, which is not common practice in wood analysis, has been successfully applied to palynological data analysis [21]. In this particular case, the components' scores characterize the spectral bands. Large positive scores indicating absorbance higher than average (i.e., highly abundant compounds) and large negative scores indicating absorbance lower than average (i.e., low abundance compounds). Thus, a "score spectra" can be constructed for each principal component and the compounds behind the combination of absorbance bands can be identified. Samples are characterized by loadings and the square of the loadings can be taken as a measure of the influence of each component (i.e., the underlying compounds) on the spectroscopic properties of each sample.

The PCA were executed using the varimax rotation, extracting five factors. PCA was first applied to data of both beam wood and shipwreck wood together, aiming to identify relevant and characteristic components. In addition, PCA was applied separately on the data obtained from the two wood pieces, to extract wood-specific variations in each type of wood.

One-way ANOVA was carried out to assess the significance of the differences between wood types and within each wood type. For the latter, measurements were grouped (4–5 consecutive positions in the wood) (B1–5 and SW1–5, Fig. 2). The classification by homogenous subsets was done by the post hoc test of Student–Newman–Keuls, with alpha = 0.05. All statistical tests were done using SPSS 20.

2.4. PY–GC/MS measurement

Pyrolysis–GC–MS was performed on small fragments of wood carved from five and three different locations on the beam wood and the shipwreck wood, respectively. Samples were embedded in quartz wool in quartz tubes. Pyrolysis was performed using a CDS 5250 at 650 °C for 20 s (10 °C ms^{-1} heating rate). Pyrolysis products were swept online into a 6890 N gas chromatograph (Agilent Technologies) using He as the carrier gas (1 ml/min), and a HP-5MS polysiloxane-based column (length 30 m; internal diameter 0.25 mm; film thickness 0.25 mm) for separation. The GC temperature program was from 50 °C (initial temperature) to 325 °C (final temperature, 5 min dwell time), at a rate of 20 °C min^{-1}. The pyrolysis products were identified using an Agilent 5975 mass spectrometer operating in 70 eV electron impact (m/z 50–500). Compound identifications were done using the NIST '05 library as well as on mass spectral data and retention time comparisons with data reported in the literature. Quantification of pyrolysis products was based on the peak area of dominant fragment ions. The relative

Table 1
Infrared bands and related molecular bonds assigned.

| Wavenumber (cm^{-1})	Bands assignments	References
1734	C=O vibration of esters, ketones, aldehydes in hemicellulose	[16,19]
1633	Absorbed O–H and conjugated C–O lignin or cellulose	[26,31]
1591	Aromatic skeletal vibration typical for S units plus C=O stretch	[6,16]
1570	Aryls or conjugated aryl groups of lignin	[23]
1504	Aromatic skeletal vibrations guaiacyl rings	[6,16]
1477	C–H asymmetric deformation in –OCH$_3$, CH$_2$ in pyran ring symmetric scissoring	[31]
1458	CH– deformation; asymmetric in plan for lignin and hemicellulose	[6,16,26]
1419	Aromatic skeletal vibration combined with CH in plane deformation for lignin and cellulose	[6,16,26]
1369	CH deformation in cellulose and hemicellulose	[26,31]
1327	C–O vibration in syringyl and guaiacyl rings, C–H cellulose	[6,26]
1263	Guaiacyl ring breathing, C–O stretch in lignin; C–O linkage in guaiacyl aromatic methoxyl groups	[26,31]
1219	C–O stretch in syringyl rings	[42]
1122	C–H vibration in lignin (typical for S units) and C–O stretching in cellulose	[31]
1024	C–O stretching in cellulose and lignin	[17,31]
985	C–O stretching in cellulose	[16]
874	C–H out of plane glucose ring in cellulose and hemicellulose and for guaiacyl rings in lignin	[12,37]
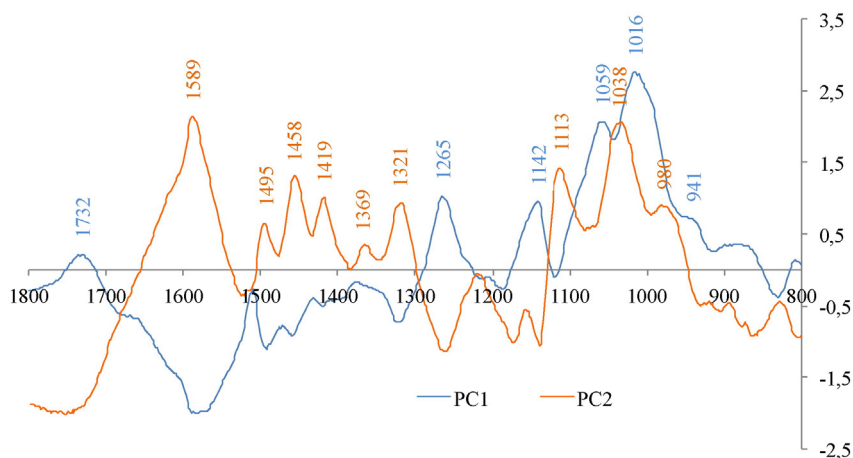
Fig. 4. PC1 (blue) and PC2 (orange) scores plot of the combined PCA (transposed matrix) for the fingerprint region of the beam and the shipwreck wood. (For interpretation of the references to color in this figure legend, the reader is referred to the web version of this article.)

proportions of each pyrolysis product were calculated as the percentage of the sum of all peak areas (total quantified peak area, TQPA).

3. Results and discussions

3.1. Characteristic FTIR spectra

The fingerprint regions of the two wood samples are shown in Fig. 3. The average and standard deviation (SD) spectra allow for a convenient description of the main FTIR characteristics of the sample sets obtained: the average spectra reflect the dominant spectral bands, while the SD spectra provide an indication of which bands exhibit the largest relative variations (i.e., those with higher SD). The average spectra of the fingerprint region of the two types of wood are rather similar as nine out of the 14 discernible bands are shared by the two types of wood. They reflect strong absorbance in the regions of bond vibrations typical of cellulose and lignin (related bands between 1507–1260 and 1059–1016 cm^{-1} and 895 cm^{-1}). Nevertheless, the SD spectra show clear differences between the two types of wood with the beam wood showing less variation than the shipwreck wood (Fig. 3). The largest absorption occurs near 1024 cm^{-1} in the beam wood and 1032 cm^{-1} in the shipwreck wood. In the former, the second region with largest variation is that between 1414 and 1477 cm^{-1}; while bands at 874, 895, 1263, 1323, 1570, 1637 and 1734 cm^{-1} presented much lower

variation. In the latter, the variability of bands 985 and 1591 cm^{-1} is quite similar to the largest one at 1032 cm^{-1} (Fig. 3); slightly lower standard deviations are shown by bands at 1122, 1219, 1419, 1458, 1504 and 1633 cm^{-1}; while the lowest variation was found in bands 874, 897, 1263, 1327 and 1369 cm^{-1}.

Table 1 presents the band assignments of the main peaks observed in the fingerprint region, between 1800 and 800 cm^{-1}. The largest values of the SD spectra are assigned to the C–O bonds (1024 and 1032 cm^{-1}) stretching usually attributed to carbohydrates [29]. In addition to that, the aromatic skeletal vibration typical of syringyl moieties (1591 cm^{-1}) is clearly discernible in the shipwreck sample, whereas vibrations of lignin (1419 and 1458 cm^{-1}) and C–H deformations of pyran rings (1477 cm^{-1}) also show a large variability in the beam wood. Of the shared bands, the relative variation at 874, 1024–1032 and 1323–1327 cm^{-1} is similar in both woods. The variability for bands at 1263, 1414–1419 and 1448–1458 cm^{-1} is higher in the beam wood; while standard deviation at 895 and 1633–1637 cm^{-1} is higher in the shipwreck wood. Apart from the peak at 1591 cm^{-1}, the shipwreck sample also shows specific bands of variation at 1122, 1219 and 1504 cm^{-1}, and the beam wood at 1570 and 1734 cm^{-1}. In terms of overall composition, the shipwreck wood is more heterogeneous than the beam wood, showing larger variability in the lignin spectroscopic signals, even though the beam wood seems to have larger variability in the cellulose/hemicelluloses composition.
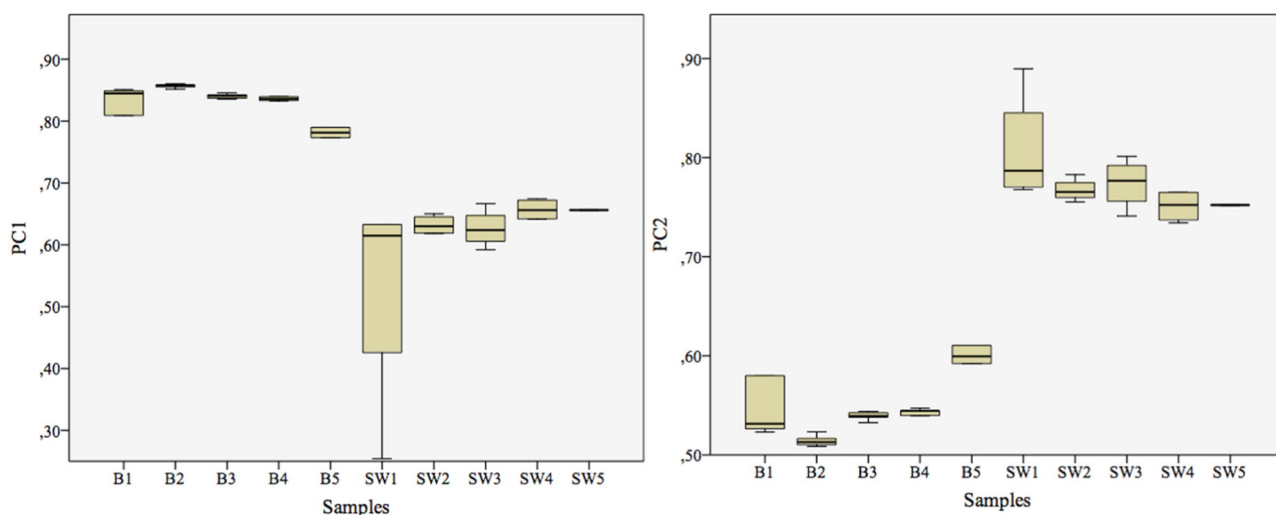

Fig. 5. Box-plot of the PC1 and PC2 loading of the two archeological woods analyzed.

Table 2
Between wood and within wood test of PC1 and PC2 loadings.

	Between B and SW		Within B		Within SW	
	F value	Pr (>F)	F value	Pr (>F)	F value	Pr (>F)
PC1	103.98	8.25×10^{-13}	4.7388	0.007	1.2761	0.329
PC2	340.58	2.20×10^{-16}	5.0831	0.005	1.9917	0.155

3.2. Principal component analysis

The two first components extracted by PCA, using the transposed matrix (PCA_t), accounted for 99% of the total variance in the whole dataset (both wood types included), of which PC1 accounted for 56% and PC2 for 43%. The PCA using the direct matrix (PCA_d) extracted five components, which account for 96% of total variance. This suggests that the PCA_t is more efficient (i.e., accounts for a slightly larger proportion of the spectroscopic information using a smaller number of components) than the PCA_d. For this reason and because of the negligible added value of the PCA_d, we focus on the results of the transposed matrix (PCA_t).

3.2.1. PCA_t of beam and shipwreck wood combined

Fig. 4 represents the partial spectra (fingerprint region) of the component scores (PC1, PC2). High positive scores at 1016 and 1059 cm^{-1} characterize PC1, moderate positive scores at 1142, 1265 and 941 cm^{-1}, a low positive score at 1732 cm^{-1} and a large negative score at 1589 cm^{-1}. PC2 is characterized by high positive scores at 1589, 1038, 1113 and 1458 cm^{-1}, moderate positive scores at 1419, 1321, 1495 and 980 cm^{-1}, a low positive score at 1369 cm^{-1} and negative scores at 1732, 1265 and 1142 cm^{-1}. Thus, PC1 shows positive high scores at the typical bands for cellulose and hemicellulose, with the C–O stretching bands exhibiting the highest scores [17,29,31]; while the absorption in PC2 is related to the aromatic skeletal vibration of lignin and to the C–O stretching for lignin with a band for C–H vibration in syringyl [16,17,20,28].

The box-plot of the loadings of the samples for the two first components (Fig. 5) shows a clear difference between the two wood types. The beam wood has higher loadings for PC1, which is related to the carbohydrate content; while the sample of the shipwreck has higher loadings for PC2, which accounts for the lignin signal. The beam wood showed a larger variation in both PC1 and PC2 than the shipwreck wood. The ANOVA test indicates that these differences in PC1 and PC2 loadings are highly significant (P < 0.01; Tables 2 and 3). Furthermore, a significant (P < 0.01) difference was also found between the inner and outer sections of the beam wood core, reflecting the radial variation in lignin content. Lourenço et al. [22] also found variations in lignin content in teak wood between sapwood and heartwood using PY–GC–MS. The shipwreck wood did not show significant differences in carbohydrate (PC1) or lignin (PC2) content between the different sections of the timber analyzed (Table 2).

These results highlight the differences in the cellulose, hemicellulose and lignin contents between softwood and hardwood species [8]. Moreover, PC1 and PC2 confirm the negative relationship between lignin and carbohydrate in lignocellulosic biomass [3,28,30,37].

3.2.2. Individual PCA_t of beam and shipwreck wood

The spectra of the PC1 and PC2 scores obtained from the separate PCA are shown in Fig. 6. The first components for both cores (PC1-B, beam; PC1-SW, shipwreck), showed very high scores (i.e., large absorbance) for the bands between 987 and 1053 cm^{-1}, and moderately high scores for bands near 862 and 899 cm^{-1}. Furthermore, PC1-B shows positive scores near 1736, 1263 and 1225 cm^{-1}, whereas PC1-SW has high positive scores at 1439 and 1309 cm^{-1}. For PC2-B, high values are observed at 1452, 1423 1026, and 874 cm^{-1}, whereas PC2-SW shows high positive scores for bands between 1026 and 1631 cm^{-1} (Fig. 6).

The bands with high positive scores in the first components of both PCA (PC1-B, PC1-SW) are related to bond vibrations in carbohydrates (between 987 and 1053 cm^{-1}), with an additional absorbance at 1736 cm^{-1} related the C=O vibration of hemicellulose, which is lower in the shipwreck wood. Hence, positive PC1 scores correspond to samples that are depleted in polysaccharides in general, and to hemicellulose in particular for the shipwreck wood. Hemicellulose is known to be sensitive to chemical degradation and the decline of its representative band at 1736 cm^{-1} was also shown for other types of ancient wood from archeological contexts [29,35]. The second component (PC2-B and PC2-SW) correspond to lignin, due to the C=C aromatic ring vibrations and also for C–O and O–H vibration in lignin [13]. In our study, relative to the beam wood, an aromatic C–H deformation of guaiacyl was found near 874 cm^{-1} as also observed by Evans [12], who observed it only in softwood. The typical C–H bond vibration in syringyl moieties was only detected in the shipwreck wood near 1124 cm^{-1}.

A further difference between the two types of wood is the functional group assignment and scores of the bands near 1263 and 1225 cm^{-1}, attributed to the deformation bonds in hemicellulose and guaiacyl in PC1-B, whereas in PC2-SW these are attributed to the deformation of lignin compounds, particularly syringyl moieties [28]. The weak absorbance of this band in PC2-B should be related to the very low amount of syringyl moieties in softwood. This highlights the differences in lignin composition between softwood and hardwood [8]. Evans [12] obtained similar results comparing softwood and hardwood, with relatively intense aromatic vibrations between 1600 and 1510 cm^{-1} in the hardwood materials.

3.3. Pyrolysis–gas chromatography–mass spectrometry

The most abundant products identified (Fig. 7, Table 4) are related to carbohydrates and lignin, which is a common feature for lignocellulosic materials pyrolysis [22,24,38,41]. The beam wood produced more carbohydrates (e.g., furans, furaldehydes, pyrans and anhydrosugars) than the shipwreck wood (Table 5), with the exception of 4-hydroxy-5,6-dihydro-(2H)-pyran-2-one. This is in agreement with the interpretation of the FTIR data. Guaiacyl lignin markers (guaiacols) were more abundant in the beam wood, whereas the syringyl lignin products were highly abundant in the shipwreck wood and negligible in the beam wood. These differences reflect the guaiacyl-based lignin in gymnosperms (pine beam wood) and the mixed guaiacyl–syringyl lignin in angiosperms (oak shipwreck wood), with a larger proportion of syringyl derivatives (see also [38]). Traces of products from other biopolymers could be identified by searching specifically for them using

Table 3
Post hoc test of Student–Newman–Keuls between and within samples.

	Between B and SW		Within B					Within SW				
	B	SW	B1	B2	B3	B4	B5	SW1	SW2	SW3	SW4	SW5
PC1	0.83[b]	0.62[a]	0.81[ab]	0.86[b]	0.84[b]	0.84[b]	0.78[a]	0.53[a]	0.63[a]	0.63[a]	0.66[a]	0.66[a]
PC2	0.55[a]	0.77[b]	0.57[ab]	0.51[a]	0.54[a]	0.54[a]	0.60[b]	0.81[a]	0.77[a]	0.77[a]	0.75[a]	0.75[a]

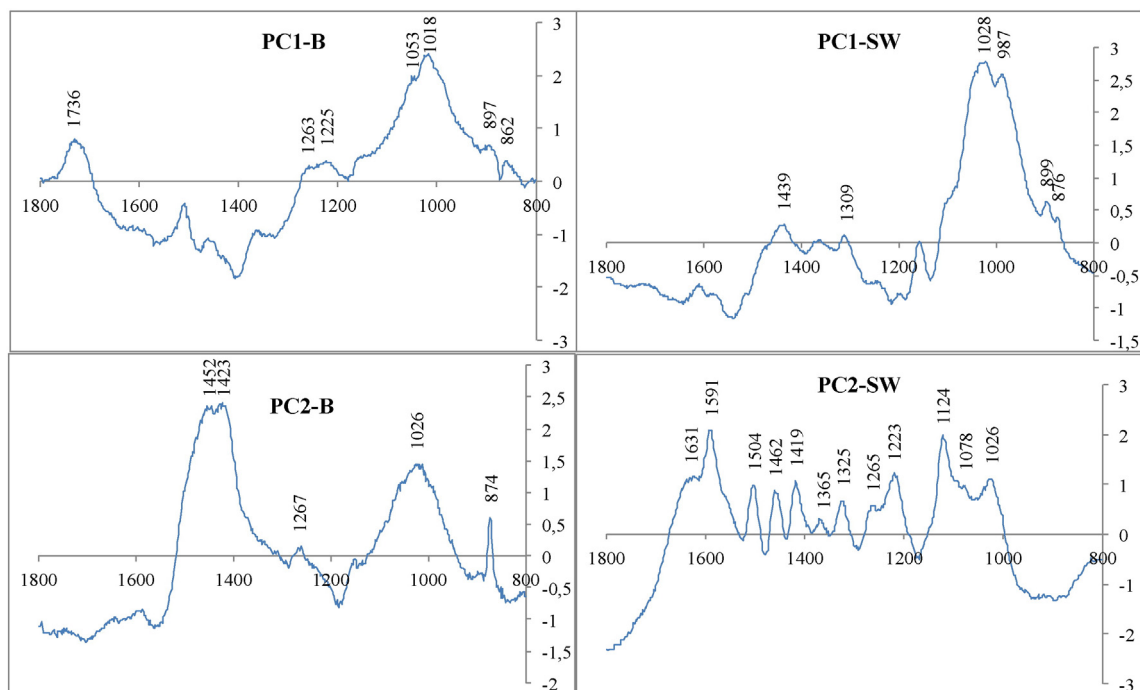Groups are classed in ascending order with the label a, b, c, ….

Fig. 6. PC1 and PC2 scores plot of the separate PCA analyses (beam wood PC1-B and PC2-B; shipwreck wood: PC1-SW and PC2-SW).

partial ion chromatograms, such as catechol (m/z 64 and 110) and 4-methylcatechol (m/z 78 and 124) from tannins, which were more abundant in the pine samples. Similarly, traces of diterpene pine resins could be identified from partial ion chromatograms of various targeted

m/z. However, these compounds were not quantified because they were not recorded by the initial screening of the major peaks. The intensity of these peaks was very low, and it seems unlikely that they represent a significant part of the biomass in any of the wood samples, which
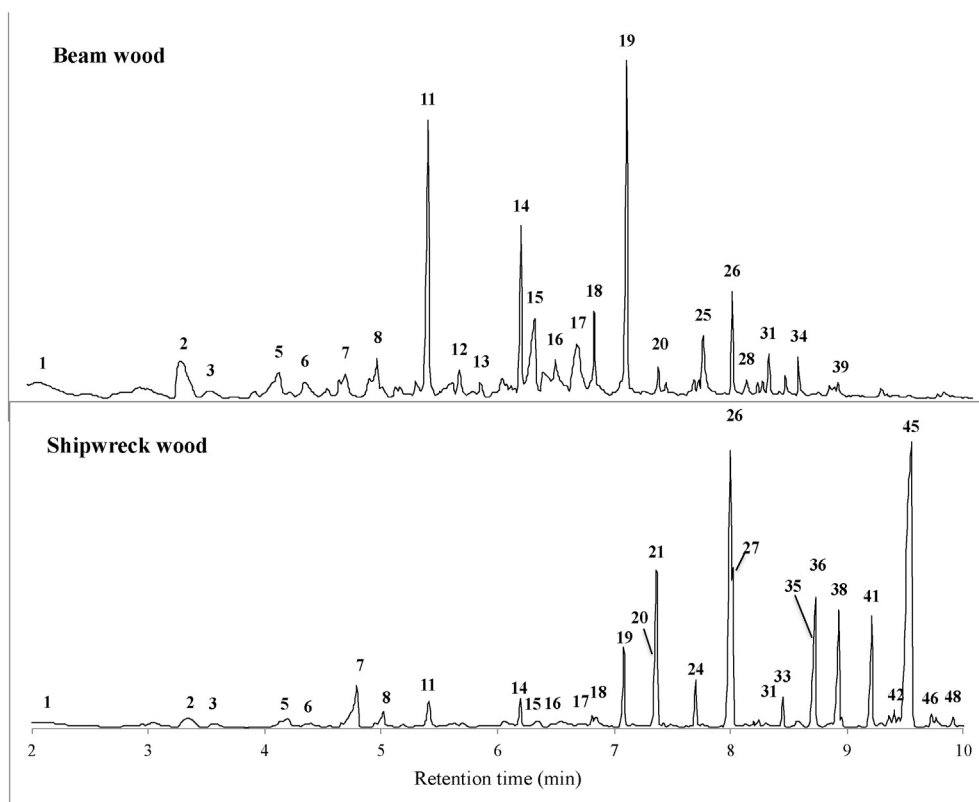

Fig. 7. Example of total ion current chromatograms of the beam wood and shipwreck wood (peak labels refer to the compound identifications in Table 5).

Table 4
Compounds identified by PY–GC–MS of the beam and shipwreck wood samples and relative proportions (expressed as % of total quantified peak area).

Pyrolysis products				Relative area (%) B sample		Relative area (%) SW sample	
No.	Name	RT (min)	m/z	Mean	SD	Mean	SD
1	2-Methylfuran	2.13	82 + 53	1.47	0.63	1.11	0.19
2	3/2-Furaldehyde	3.32	95 + 96	8.09	3.43	4.42	0.86
3	Cyclopentenone compound	3.55	53 + 98	1.53	0.68	0.50	0.08
4	4-Cyclopenten-1.3-dione	3.76	68 + 96	0.36	0.09	0.21	0.03
5	2.3-Dihydro-5.6-methylfuran-2-one	4.15	55 + 98	9.94	3.75	3.43	0.39
6	5-Methyl-2-furaldehyde	4.38	53 + 110	0.97	0.56	0.52	0.11
7	4-Hydroxy-5.6-dihydro-(2H)-pyran-2-one	4.72	58 + 114	3.90	2.25	8.11	1.63
8	3-Hydroxy-2-methyl-2-cyclopenten-1-one	4.97	55 + 112	2.87	0.74	1.53	0.17
9	2/3-Methylphenol	5.12	107 + 108	0.12	0.09	0.06	0.04
10	4-Methylphenol	5.29	107 + 108	0.25	0.18	0.13	0.07
11	Guaiacol	5.39	109 + 124	10.22	2.68	1.66	0.26
12	Levoglucosenone	5.66	68 + 98	0.52	0.37	0.12	0.04
13	3-Hydroxy-2-methyl-4h-pyran-4-one	5.66	126	0.57	0.25	0.23	0.04
14	4-Methylguaiacol	6.18	123 + 138	4.54	2.46	1.27	0.32
15	Dianhydro-alpha-D-glucopyranose	6.30	57 + 69	3.10	2.01	0.62	0.10
16	5-Hydroxymethyl-2-furancarboxaldehyde	6.51	69 + 57	1.07	0.54	1.00	0.10
17	3-Hydroxy-2-methyl-4h-pyran-4-one	6.67	97 + 126	2.47	2.04	1.28	0.33
18	4-Ethylguaiacol	6.80	137 + 152	1.76	0.71	0.47	0.15
19	4-Vinylguaiacol	7.07	135 + 150	11.80	3.15	3.30	0.39
20	4-(prop-1-enyl) guaiacol	7.35	164 + 149	0.67	0.29	1.19	0.18
21	Syringol	7.35	154 + 139	0.00	0.00	5.75	0.77
22	4-Propylguaiacol	7.41	137 + 166	0.29	0.06	0.19	0.02
23	x-Methylguaiacol	7.64	123 + 138	0.24	0.22	0.10	0.08
24	4-(Prop-2-enyl) guaiacol (cis)	7.69	164 + 149	0.39	0.14	0.73	0.15
25	4-Formylguaiacol (vanillic aldehyde)	7.71	151 + 152	3.05	0.51	0.23	0.02
26	4-(Prop-2-enyl) guaiacol (trans)	7.98	164 + 149	3.94	2.02	7.82	1.56
27	4-Methylsyringol	8.00	168 + 153	0.00	0.00	2.13	3.37
28	Unidentified (homovanillin?)	8.09	137 + 166	1.04	0.33	0.26	0.05
29	C$_3$H$_3$-guaiacol	8.19	147 + 162	0.46	0.30	0.18	0.02
30	C$_3$H$_3$-guaiacol	8.23	147 + 162	0.38	0.20	0.17	0.02
31	4-Acetylguaiacol	8.28	151 + 166	1.20	0.14	0.54	0.05
32	Vanillic acid methyl ester	8.42	151 + 182	0.38	0.12	0.46	0.05
33	4-Ethylsyringol	8.45	167 + 182	0.00	0.00	1.23	0.13
34	4-(Propan-2-one) guaiacol	8.54	137 + 180	1.73	0.30	0.44	0.04
35	4-Vinylsyringol	8.70	180	0.00	0.00	4.83	0.47
36	4-(Propan-2-one) guaiacol	8.81	137 + 180	0.32	0.12	6.97	0.64
37	4-(Propan-1-one) guaiacol	8.86	151 + 180	0.48	0.29	0.16	0.03
38	4-(Prop-1-enyl) syringol	8.93	194 + 179	0.00	0.00	2.41	0.15
39	4-Propylsyringol	8.95	167 + 196	0.00	0.00	0.41	0.03
40	Dihydroconiferyl alcohol	9.25	137 + 182	0.65	0.24	0.19	0.06
41	4-(Prop-2-enyl) syringol (cis)	9.21	194 + 179	0.00	0.00	2.57	0.21
42	Syringaldehyde	9.36	182 + 181	0.00	0.00	0.58	0.08
43	C$_3$H$_3$-syringol	9.41	192 + 177	0.00	0.00	0.37	0.09
44	C$_3$H$_3$-syringol	9.45	192 + 177	0.00	0.00	0.19	0.07
45	4-(Prop-2-enyl) syringol (trans)	9.55	194 + 179	0.00	0.00	21.16	1.18
46	4-Acetylsyringol	9.72	181 + 196	0.02	0.04	0.79	0.22
47	Trans-coniferaldehyde	9.75	178	0.37	0.27	0.16	0.04
48	4-(Propan-2-one) syringol	9.91	167 + 210	0.02	0.03	0.65	0.29

implies that the interpretation of the FTIR spectra, at least of PC1 and PC2, can be safely associated with carbohydrates and lignin, without risking interference from tannin or resin constituents.

Despite the significant depletion of carbohydrates in the shipwreck wood, the lignin fingerprint is that of a typical well-preserved hardwood, with large proportions of syringols with 4-propenyl side chains, the trans-stereoisomer of 4-(prop-2-enyl) syringol in particular (Table 4). Analogously, the abundance of 4-propenylguaiacols in the beam wood samples analyzed indicates that the lignin is well-

Table 5
Average of total abundance of carbohydrates and guaiacyl (G) and syringyl (S) lignin of the beam and shipwreck woods.

		Building (pine) %	Shipwreck (oak) %
Carbohydrate	Total	47.07	24.73
Lignin	G	43.26	26.33
	S	0.68	43.27
	S + G	43.94	69.60
	S / G	0.02	1.64

preserved. Hence, the level of interference of such polymers in the FTIR signal and therefore erroneous band assignment should be limited.

3.4. Effect of environment conditions on archeological wood

Differences in wood composition between the beam and the shipwreck wood can be attributed to differences in wood chemistry between softwood and hardwood (pine vs. oak), in combination with diagenesis processes related to the environment conditions (oxic vs. anoxic environment). The higher proportion of carbohydrate compounds in the beam wood could indicate preferential degradation of polysaccharides in the shipwreck wood. This probably explains why lignin was more abundant in the shipwreck timber, even though a combined source and environment effect cannot be ruled out. Previous FTIR studies showed that lignin is partially oxidized when wood is under dry air conditions during a long period, causing an increase in the relative proportion of carbonyl groups [5,39]. However, wood under anoxic conditions may undergo hydrolysis followed by leaching of the hydrophilic carbohydrates, contributing to the dominance of the lignin proportion

[5,9,10,39]. Gelbrich et al. [15] also found a high degree of degradation of archeological wood, average lignin content increasing from 25% in fresh wood to up to 45% in archeological wood.

4. Conclusions

The application of PCA on transposed FTIR data matrices highlighted the differences in chemical composition between the two archeological woods. The beam wood showed a higher content of carbohydrates whereas the shipwreck wood contained more lignin. The ANOVA test confirmed that these differences between wood types are significant; it also shown that there are significant within-wood variations in lignin content in the beam wood. The FTIR results were in agreement with PY–GC–MS analyses of selected samples, showing that the woods are composed predominantly of carbohydrates (polysaccharides) and different lignin types, and that the oak-derived shipwreck wood contains more lignin and particularly more syringyl lignin than the pine-derived beam wood. The observed differences between woods may be due to the fact that they originate from different sources (pine and oak), which differ in their cellulose, hemicellulose and lignin contents. But, at least in part, they may have arisen as a consequence of wood degradation due to the different environments under which they were subjected for several centuries (oxic vs. anoxic) as well. In conclusion, the possibility of extracting meaningful information on wood chemistry using FTIR in combination with multivariate statistics, together with the significant within-wood differences (for softwood), and the excellent preservation state of the lignin in the archeological wood analyzed, suggest that this approach can become a useful tool in wood provenance studies.

Acknowledgments

References

[1] G.G. Allison, Application of Fourier Transform Mid-Infrared Spectroscopy (FTIR) for Research Into Biomass Feed-Stock, Fourier Transforms—New Analytical Approaches and FTIR Strategies, in: Goran Nikolic (Ed.), ISBN: 978-953-307-232-6, 2011.
[2] W.B. Banks, N.L. Owen, FTIR studies of hydrophobic layers on wood, Spectrochim. Acta A 43 (1987) 1527–1533.
[3] F. Bertaud, B. Holmbom, Chemical composition of earlywood and latewood in Norway spruce heartwood, sapwood and transition zone wood, Wood Sci. Technol. 38 (2004) 245–256.
[4] R. Bodirlau, C.A. Teaca, Fourier transform infrared spectroscopy and thermal analysis of lignocelluloses fillers treated with organic anhydrides, Rom. J. Phys. 54 (1–2) (2009) 93–104.
[5] B.K. Borgin, O. Faix, W. Schweers, The effect of aging on lignins of wood, Wood Sci. Technol. 9 (1975) 207–211.
[6] H. Chen, C. Ferrari, M. Angiuli, J. Yao, C. Raspi, E. Bramanti, Qualitative and quantitative analysis of wood samples by Fourier transform infrared spectroscopy and multivariate analysis, Carbohydr. Polym. 82 (2010) 772–778.
[7] X. Colom, F. Carrillo, F. Nogués, P. Garriga, Structural analysis of photodegraded wood by means of FTIR spectroscopy, Polym. Degrad. Stab. 80 (2003) 543–549.
[8] X. Colom, F. Carrillo, Comparative study of wood samples of the northern area of Catalonia by FTIR, J. Wood Chem. Technol. 25 (2005) 1–11.
[9] M.P. Colombini, M. Orlandi, F. Modugno, E.L. Tolppa, M. Sardelli, L. Zoia, C. Crestini, Archaeological wood characterization by PY/GC/MS, GC/MS, NMR and GPC techniques, Microchem. J. 85 (2007) 164–173.
[10] M.P. Colombini, J.J. Lucejko, F. Modugno, M. Orlandi, E.L. Tolppab, L. Zoia, A multi-analytical study of degradation of lignin in archaeological waterlogged wood, Talanta 80 (2009) 61–70.
[11] B. Esteves, A.V. Marques, I. Domingos, H. Pereira, Chemical changes of heat treated pine and eucalypt wood monitored by FTIR, Maderas-Cienc. Tecnol. 15 (2013) 245–258.
[12] P.A. Evans, Differentiating "hard" from "soft" woods using Fourier transform infrared and Fourier transform Raman spectroscopy, Spectrochim. Acta A Mol. 47 (1991) 1441–1447.
[13] O. Faix, J. Bremer, O. Schmidt, J.T. Stevanovic, Monitoring of chemical changes in white-rot degraded beech wood by pyrolysis–gas chromatography and Fourier-transform infrared spectroscopy, J. Anal. Appl. Pyrol. 21 (1991) 147–162.
[14] O. Faix, J.H. Bottcher, The influence of particle size and concentration in transmission and diffuse reflectance spectroscopy of wood, Holz Roh Werkst. 50 (1992) 221–226.
[15] J. Gelbrich, C. Mai, H. Militz, Chemical changes in wood degraded by bacteria, Int. Biodeterior. Biodegrad. 61 (2008) 24–32.
[16] R. Herrera, X. Erdocia, R. Llano-Ponte, J. Labidi, Characterization of hydrothermally treated wood in relation to changes on its chemical composition and physical properties, J. Anal. Appl. Pyrol. 107 (2014) 256–266.
[17] R. Hori, J. Sugiyama, A combined FT-IR microscopy and principal component analysis on softwood cell walls, Carbohydr. Polym. 52 (2003) 449–453.
[18] N. Labbé, D. Harper, T. Rials, Chemical structure of wood charcoal by infrared spectroscopy and multivariate analysis, J. Agric. Food Chem. 54 (2006) 3492–3497.
[19] Z.H. Li, N. Labbé, S.G. Driese, H.D. Grissino-Mayer, Micro-scale analysis of tree-ring $\delta^{18}O$ and $\delta^{13}C$ on α-cellulose spline reveals high-resolution intra-annual climate variability and tropical cyclone activity, Chem. Geol. 284 (2011) 138–147.
[20] Q. Liu, S. Wang, Y. Zheng, Z. Luo, K. Cen, Mechanism study of wood lignin pyrolysis by using TG–FTIR analysis, J. Anal. Appl. Pyrol. 82 (2008) 170–177.
[21] L. López-Merino, N. Silva Sánchez, J. Kaal, J.A. López-Sáez, A. Martínez Cortizas, Post-disturbance vegetation dynamics during the Late Pleistocene and the Holocene: an example from NW Iberia, Glob. Planet. Chang. 92–93 (2012) 58–70.
[22] A. Lourenço, D.M. Neiva, J. Gominho, A.V. Marques, H. Pereira, Characterization of lignin in heartwood, sapwood and bark from *Tectona grandis* using Py–GC–MS/FID, Wood Sci. Technol. 49 (2015) 159–175.
[23] J. Lojewska, P. Miskowiec, T. Lojewski, L.M. Proniewicz, Cellulose oxidative and hydrolytic degradation: in situ FTIR approach, Polym. Degrad. Stab. 88 (2005) 512–520.
[24] J.J. Łucejko, F. Modugno, E. Ribechini, J.C. Del Río, Characterisation of archaeological waterlogged wood by pyrolytic and mass spectrometric techniques, Anal. Chim. Acta 654 (2009) 26–34.
[25] A.K. Moore, N.L. Owen, Infrared spectroscopic studies of solid wood, Appl. Spectrosc. Rev. 36 (2001) 65–86.
[26] G. Müller, C. Schöpper, H. Vos, A. Kharazipour, A. Polle, FTIR–ATR spectroscopic analyses of changes in wood properties during particle- and fibreboard production of hard- and softwood trees, BioResources 4 (2009) 49–71.
[27] K.K. Pandey, A study of chemical structure of soft and hardwood and wood polymers by FTIR spectroscopy, J. Appl. Polym. Sci. 71 (1999) 1969–1975.
[28] K.K. Pandey, A.J. Pitman, FTIR studies of the changes in wood chemistry following decay by brown-rot and white-rot fungi, Int. Biodeterior. Biodegrad. 52 (2003) 151–160.
[29] M. Picollo, E. Cavallo, N. Macchioni, O. Pignatelli, B. Pizzo, I. Santoni, Spectral Characterization of Ancient Wooden Artefacts With the Use of Traditional IR Techniques and ATR Device: A Methodological Approach, E-preservation Science Morana RTD, Slovenia, 2011 (ISSN: 1581–9280).
[30] B. Pizzo, E. Pecoraro, A. Alves, N. Macchioni, J.C. Rodrigues, Quantitative evaluation by attenuated total reflectance infrared (ATR–FTIR) spectroscopy of the chemical composition of decayed wood preserved in waterlogged conditions, Talanta 131 (2015) 14–20.
[31] C.M. Popescu, M.C. Popescu, G. Singurel, C. Vasile, D.S. Argyropoulos, S. Willfor, Spectral characterization of eucalyptus wood, Appl. Spectrosc. 61 (2007) 1168–1177.
[32] C.M. Popescu, M.C. Popescu, G. Singurel, C. Vasile, Structural changes in biodegraded lime wood, Carbohydr. Polym. 79 (2010) 362–372.
[33] R. Rana, G. Müller, A. Naumann, A. Polle, FTIR spectroscopy in combination with principal component analysis or cluster analysis as a tool to distinguish beech (*Fagus sylvatica* L.) trees grown at different sites, Holzforschung 62 (2008) 530–538.
[34] C. Saiz-Jiménez, J.W. Leeuw, Lignin pyrolysis products: their structures and their significance as biomarkers, Org. Geochem. 10 (1986) 869–876.
[35] A. Sandak, J. Sandak, L. Babinski, D. Pauliny, M. Riggio, Spectral analysis of changes to pine and oak wood natural polymers after short-term waterlogging, Polym. Degrad. Stab. 99 (2014) 68–79.
[36] I. Santoni, E. Callone, A. Sandak, J. Sandak, D. Dirè, Solid state NMR and IR characterization of wood polymer structure in relation to tree provenance, Carbohydr. Polym. 117 (2015) 710–721.
[37] D.L. Sills, J.M. Gossett, Using FTIR to predict saccharification from enzymatic hydrolysis of alkali pretreated biomasses, Biotechnol. Bioeng. 109 (2012) 353–362.
[38] P.F. Van Bergen, I. Poole, T.M.A. Ogilvie, C. Caple, R.P. Evershed, Evidence for demethylation of syringyl moieties in archaeological wood using pyrolysis–gas chromatography/mass spectrometry, Rapid Commun. Mass Spectrom. 14 (2000) 71–79.
[39] A.W. Wilson, I.M. Godfrey, J.V. Hanna, R.A. Quezada, K.S. Finnie, The degradation of wood in old Indian Ocean shipwrecks, Org. Geochem. 20 (1993) 599–610.
[40] F. Xu, J. Yu, T. Tesso, F. Dowell, D. Wang, Qualitative and quantitative analysis of lignocellulosic biomass using infrared techniques: a mini-review, Appl. Energy 104 (2013) 801–809.
[41] H. Yang, Y. Huang, Q. Leng, B.A. LePage, C.J. Williams, Biomolecular preservation of Tertiary *Metasequoia* fossil Lagerstätten revealed by comparative pyrolysis analysis, Rev. Palaeobot. Palynol. 134 (2005) 237–256.
[42] J. Zhao, W. Xiuwen, J. Hu, Q. Liu, D. Shen, R. Xiao, Thermal degradation of softwood lignin and hardwood lignin by TG–FTIR and Py–GC/MS, Polym. Degrad. Stab. 108 (2014) 133–138.